Implications of Intercellular Signaling for Radiation Therapy: A Theoretical Dose-Planning Study

McMahon, S. J., McGarry, C. K., Butterworth, K. T., O'Sullivan, J. M., Hounsell, A. R., & Prise, K. M. (2013). Implications of Intercellular Signaling for Radiation Therapy: A Theoretical Dose-Planning Study. International journal of radiation oncology, biology, physics, 87(5), 1148-1154. DOI: 10.1016/j.ijrobp.2013.08.021

Published in:
International journal of radiation oncology, biology, physics

Implications of Intercellular Signalling for Radiation Therapy: A Theoretical Dose-Planning Study

Stephen J. McMahon, Ph.D.*, Conor K. McGarry, Ph.D.*†, Karl T. Butterworth, Ph.D.*,

Joe M. O'Sullivan, FRR(RCSI)*‡, Alan R. Hounsell, Ph.D.*†, and Kevin M. Prise, Ph.D.*

*Centre for Cancer Research and Cell Biology, Queen's University Belfast, Belfast, Northern Ireland, United Kingdom;

†Radiotherapy Physics, Northern Ireland Cancer Centre, Belfast Health and Social Care Trust, Northern Ireland, United Kingdom;

‡Clinical Oncology, Northern Ireland Cancer Centre, Belfast Health and Social Care Trust, Belfast, Northern Ireland, United Kingdom

Published as:

Implications of Intercellular Signalling for Radiation Therapy: A Theoretical Dose-Planning Study, McMahon et al, International Journal Of Radiation Oncology, Biology, Physics; 2013 87:5, 1148-1154

Summary

There is increasing evidence *in vitro* that intercellular communication plays a significant role in radiation response. However, it has not yet been established if these *in vitro* results can be reconciled with established clinical knowledge. Here, a series of prostate radiotherapy treatment plans were assessed using a theoretical model of radiation response incorporating intercellular communication, to evaluate possible impacts of signalling and highlight areas for future investigation.

Abstract

Purpose

Recent *in vitro* results have shown significant contributions to cell killing from signalling effects at doses which are typically used in radiotherapy. This study investigates whether these *in vitro* observations can be reconciled with *in vivo* knowledge and how signalling may impact on future developments in radiotherapy.

Methods and Materials

Prostate cancer treatment plans were generated for a series of 10 patients, using 3D Conformal Therapy, Intensity Modulated Radiotherapy and Volumetric Modulated Arc Therapy techniques. These plans were evaluated using mathematical models of survival following modulated radiation exposures which were developed from *in vitro* observations and incorporate the effects of intercellular signalling. The impact on dose volume histograms and mean doses were evaluated by converting these survival levels into “signalling-adjusted doses” for comparison.

Results

Inclusion of intercellular communication leads to significant differences between the signalling-adjusted and physical doses across a large volume. Organs in low-dose regions near target volumes see the largest increases, with mean signalling-adjusted bladder doses increasing from 23 to 33 Gy in IMRT plans. By contrast, in high dose regions there is a small decrease in signalling-adjusted dose, due to reduced contributions from neighbouring cells, with PTV mean doses falling from 74 to 71 Gy in IMRT. Overall, however, the dose distributions remain broadly similar, and comparisons between the

treatment modalities are largely unchanged whether physical or signalling-adjusted dose is compared.

Conclusions

Although incorporating cellular signalling significantly affects cell killing in low-dose regions and suggests a different interpretation for many phenomena, their effect in high dose regions for typical planning techniques is comparatively small. This indicates that the significant signalling effects observed *in vitro* are not contradicted by comparison with clinical observations. Future investigations are needed to validate these effects *in vivo* and to quantify their ranges and potential impact on more advanced radiotherapy techniques.

Introduction

Recent years have seen dramatic improvements in the technical delivery of radiotherapy, with sophisticated techniques like Intensity Modulated Radiotherapy (IMRT) and Volumetric Modulated Arc Therapy (VMAT) providing superior conformation of dose to target volumes while sparing surrounding healthy tissue. These techniques offer many more degrees of freedom than older techniques, allowing for sophisticated optimisation of dose delivery.

An important question raised by this increased flexibility is how to define “optimum” dose delivery. Most radiotherapy plans are currently designed with the goal of delivering a high, uniform dose to the target volume and minimising dose delivered to surrounding organs at risk. Improvements in dose delivery are thus typically used to improve dose conformation to target volumes, possibly by reducing margins. However, there is also increasing interest in “dose-painting” techniques, where inhomogeneous doses are delivered to the target volume, specifically targeting high-risk regions of the tumour volume (e.g. characterised by hypoxia or high levels of proliferation), which may be identified through the use of functional imaging (1). One of the key assumptions underlying both of these approaches is that the survival of a population of cells is determined by the dose received by that population.

However, a series of recent investigations of the response of cell populations to modulated fields has shown that their survival depends not only on the dose they experience but also on that delivered to neighbouring populations (2, 3). These effects have been attributed to intercellular communication, often termed “bystander” effects (4). Bystander effects are typically associated with cell populations exposed to extremely low doses, such as those which are completely shielded *in vitro*, or wholly outside treatment fields and exposed only

to scattered radiation amounting to a few percent of the treatment dose *in vivo,* More recently, however, analysis by several groups (5–7) has suggested that these signals are not only significant in regions which are completely outside treatment fields (“out-of-field” regions), but also play a role in the survival of cells exposed to higher doses. These can be not only in organs at risk which are exposed to a low dose (e.g. 0.5 to 1 Gy per fraction) due to being traversed by a single treatment field, but even within the high-dose regions of the target itself which are exposed to doses of several Gy per fraction(8).

These results present a strikingly different interpretation of many basic radiobiological data and suggest there is value in assessing the impact of these effects in clinical scenarios. This is further emphasised by *in vivo* observation of significant out-of-field toxicity and second cancer induction in animals exposed to modulated radiation exposures (9). It is important to note, however, that established practice in clinical radiotherapy and radiation protection is primarily based around the evaluation of physical doses, and this has useful (albeit imperfect) predictive power. Accordingly, any description of radiation response which incorporates these signalling factors must be compatible with established clinical observations, as they implicitly incorporate any underlying biology.

This work presents an initial assessment of the impact of intercellular communication on a series of prostate radiotherapy treatment plans. This approach is based on a recently published theoretical model which describes radiation response incorporating both direct damage and that resulting from intercellular signalling.(6, 7). Evaluating these effects for a series of delivery techniques and signal ranges is an important first step in understanding the *in vivo* impact of the signalling effects which are observed *in vitro*, as significant divergences between the model's predictions and clinical observations would indicate an incompatibility of the model with *in vivo* conditions.

Materials and Methods

Cellular Response Model

This work builds on previously published models which describe cellular responses to modulated radiation fields incorporating cell cycling, cell arrest, and DNA damage induced both by direct radiation exposure and indirect, cell-signalling mediated effects. It is reviewed briefly below for completeness, with full descriptions of the model and its validation in *in vitro* systems published elsewhere (6, 7, 10).

In this model, cells experience damage from two sources – direct radiation and intercellular communication – which is accumulated as a number of discrete "hits", representing damage to the cell. For direct radiation exposures, the mean number of hits induced per cell is directly proportional to the delivered dose, and are taken to be Poisson-distributed throughout the population.

This direct damage is combined with damage resulting from responses to intercellular communication. It is assumed that cells exposed to ionising radiation begin to secrete a signalling molecule responsible for these damaging effects, and continue to do so for a time proportional to the delivered dose (i.e. $t = \gamma D$). The signals are taken to be unstable, decaying with decay constant λ, and so the signal concentration (ρ) initially builds up to an equilibrium value before decaying away as cells cease signalling, schematically illustrated in Figure 1.

Bystander responses are mediated by a threshold concentration (ρ_t), below which no response occurs, and above which response is induced at a constant rate. Thus, the probability of a cell experiencing a bystander response is given by $P_B = 1 - e^{-\kappa\tau}$, where τ is the total time for which the cell is exposed to a signal above the threshold value, and κ is a

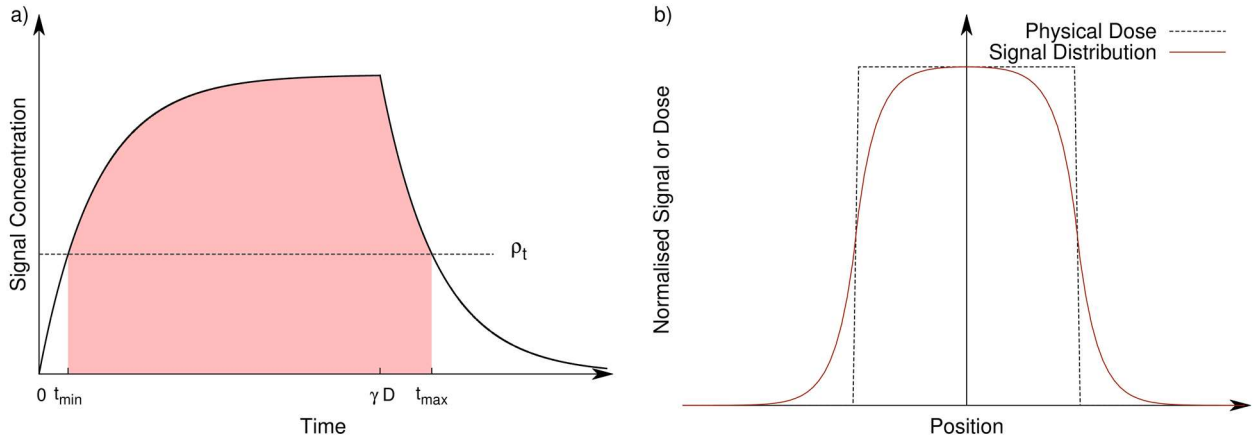

***Figure 1**: Schematic illustration of signalling kinetics. Left: Illustration of average signal concentration in a population uniformly irradiated to a dose D at time 0. Signal is produced by the cells and approaches equilibrium with signal decay until a time γD, when the irradiated cells cease signalling and the signal decays away. Bystander response is determined by* $\tau = t_{max} - t_{min}$ *, the time for which the signal level is above the response threshold* ρ_t*. Right: Illustration of equilibrium signal distribution around an idealised rectangular beam. Even for a perfectly sharp beam, diffusion can lead to significant changes in equilibrium signal levels at the margins, which can translate into differences in bystander response.*

characteristic of the cell line. Cells undergoing a bystander response see the induction of additional damage, Poisson-distributed around a mean of H_B, again a characteristic of the cell line.

Following radiation exposure, a cell population would thus have accumulated damage due to both direct and indirect effects. This damage is then related to cell cycling and arrest checkpoints, which can be calculated either on a cell-by-cell basis (6, 10), or using population-level statistics (7), to produce predictions of survival which can be compared to experimental results.

Signalling in Three-Dimensional Tissues

In *in vitro* experiments, cells are typically maintained within a growth medium which allows for extremely rapid signal diffusion, removing any significant spatial effects. However, any signalling molecules which are produced *in vivo* must propagate through tissue, traversing cells and the intercellular matrix, which is known to significantly reduce their diffusion

coefficient (11) and propagation.

As *in vivo* signal propagation is a complex, inhomogeneous phenomenon influenced by the structure, composition and vasculature of different tissues, a full description of this behaviour is outside the scope of this work. Instead, signal propagation is here modelled as a simple homogeneous diffusion process. While this is necessarily a simplification of the true behaviour, it provides a useful starting point for evaluating the compatibility of intercellular communication models with established *in vivo* knowledge and preliminary quantifications of their biological significance.

The signal diffusion is implemented in a numerical model, dividing the volume under consideration into a series of voxels (each containing uniform signal concentration) in three dimensions, with signal spreading according to the diffusion equation,

$$\frac{d\rho}{dt} = -D\nabla^2\rho$$

where D is the diffusion coefficient, ρ is the local signal concentration at each point, and ∇^2 is the Laplacian operator.

The simulation begins from a time t=0 when radiation is delivered and proceeds in a series of time-steps. At each timestep, from t to t+Δt, the signal evolves as follows:

1. Additional signal is produced within voxels, if they have been exposed to a dose sufficient that t<γD;
2. Signal diffuses between adjacent voxels, according to the diffusion equation;
3. A portion of the signal decays, determined by the characteristic decay coefficient, λ.

This model proceeds until all cells have stopped signalling and the maximum concentration in the simulation has fallen below the response threshold. For each voxel, the level of bystander response is determined by the length of time, τ, it was exposed to

signals above the response threshold, ρ_t, as outlined above. An illustration of the signal distribution and resulting exposure time is shown in Figure 1.

Once the signalling simulation is completed, the total level of damage in each voxel is calculated by combining direct and signalling-induced damage, and survival is calculated based on population-level statistics, as mentioned above (7). For comparison with physical dose in treatment plans, this survival is then converted into a “signalling-adjusted” dose (D_s) by calculating the uniform physical dose which would lead to the same level of survival.

Analysis of Bystander Signalling

Plans were created using CT datasets of ten successive prostate cancer patients (Ethics REC ref 09/NIR02/28). 3D-Conformal, IMRT and VMAT plans were designed for delivery on a Varian 2100CD linear accelerator using 6 MV photons, with a prescribed target dose of 74 Gy, delivered in 37 fractions of 2 Gy across 7.5 weeks. Target volumes and organs at risk were delineated according to the CHHiP protocol (12). Further detail on planning techniques used can be found elsewhere (13). Treatment delivery time is neglected in this analysis, as they are significantly shorter than the typical timescales associated with bystander responses (14, 15).

In addition to the physically planned dose, signalling-adjusted dose distributions were calculated for each treatment plan. All cells were modelled using parameters describing human fibroblast AGO-1522 cells (7), according to the methods outlined above. This cell line was selected as an example of normal cell response, but fitting parameters for a range of other cell types lead to similar conclusions to those presented here.

One parameter which remains uncertain from *in vitro* measurements is the diffusion coefficient, D. While this is likely to depend on tissue type, structure and vasculature,

isotropic diffusion has been assumed here as these variations are currently poorly quantified. Here, the diffusion coefficient has been quantified in terms of its one dimensional equilibrium range, $r = \sqrt{D/\lambda}$. Signalling-adjusted dose distributions were calculated for each plan for values of *r* varying from 0 to 20 mm. Although the upper limit was constrained by computational performance considerations, it encompasses a reasonable range for isotropic diffusion, with longer ranges likely involving some form of active transport, which is outside the scope of this work.

Mean organ doses and Equivalent Uniform Doses (EUD) were calculated under each condition to enable comparison of the impact of bystander signalling processes for different organs and treatment modalities. EUDs were calculated through DVH reduction (16), according to the relationship $EUD = \left(\sum D_i^{\frac{1}{n}} v_i\right)^n$, where v_i is the fraction of the organ exposed to a dose D_i, and *n* is an organ-specific scaling parameter.

Results

Impact on Dose Distributions

Figure 2 presents an illustrative slice from an IMRT prostate treatment plan, showing the physical dose distribution and the predicted changes in signalling-adjusted dose for a signal range of 15 mm. As expected, intercellular signalling leads to increased cell killing in out-of-field areas near steep dose gradients, and thus higher signalling-adjusted doses. It can also be seen that in regions of high local dose (primarily within beams), there is a reduction in signalling-adjusted dose due to more rapid signal fall-off than expected in a uniform exposure. However, this effect is relatively small, with reductions of less than 4 Gy on a 74 Gy plan, compared to increases of up to 25 Gy. Similar results were observed for

CRT and VMAT plans, which are illustrated in supplementary figure e1.

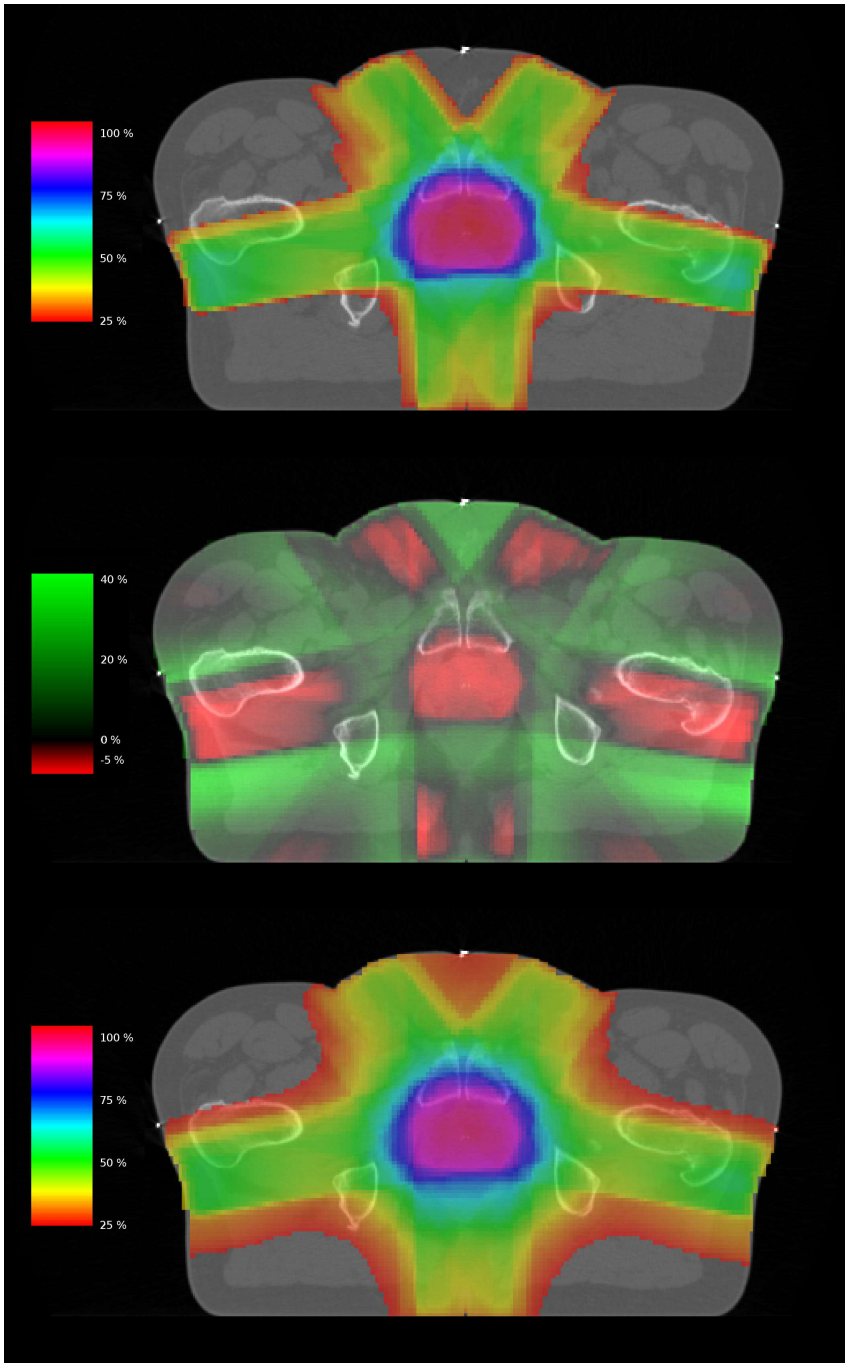

Figure 2: *Impact of bystander signalling on dose distributions for an example IMRT prostate cancer treatment plan, with a signal range of 15 mm. Top: Physical dose distribution generated by the treatment planning system. Middle: Heat-map indicating change between physical and signalling-adjusted dose. Green indicates regions which see increases in cell killing compared to physical dose alone, while red shows reduced killing. Bottom: Resulting signalling-adjusted dose plans. Directly exposed areas see a small reduction (< 5% of prescribed dose), while areas near beams see substantial increases (up to 30 % of prescribed dose).*

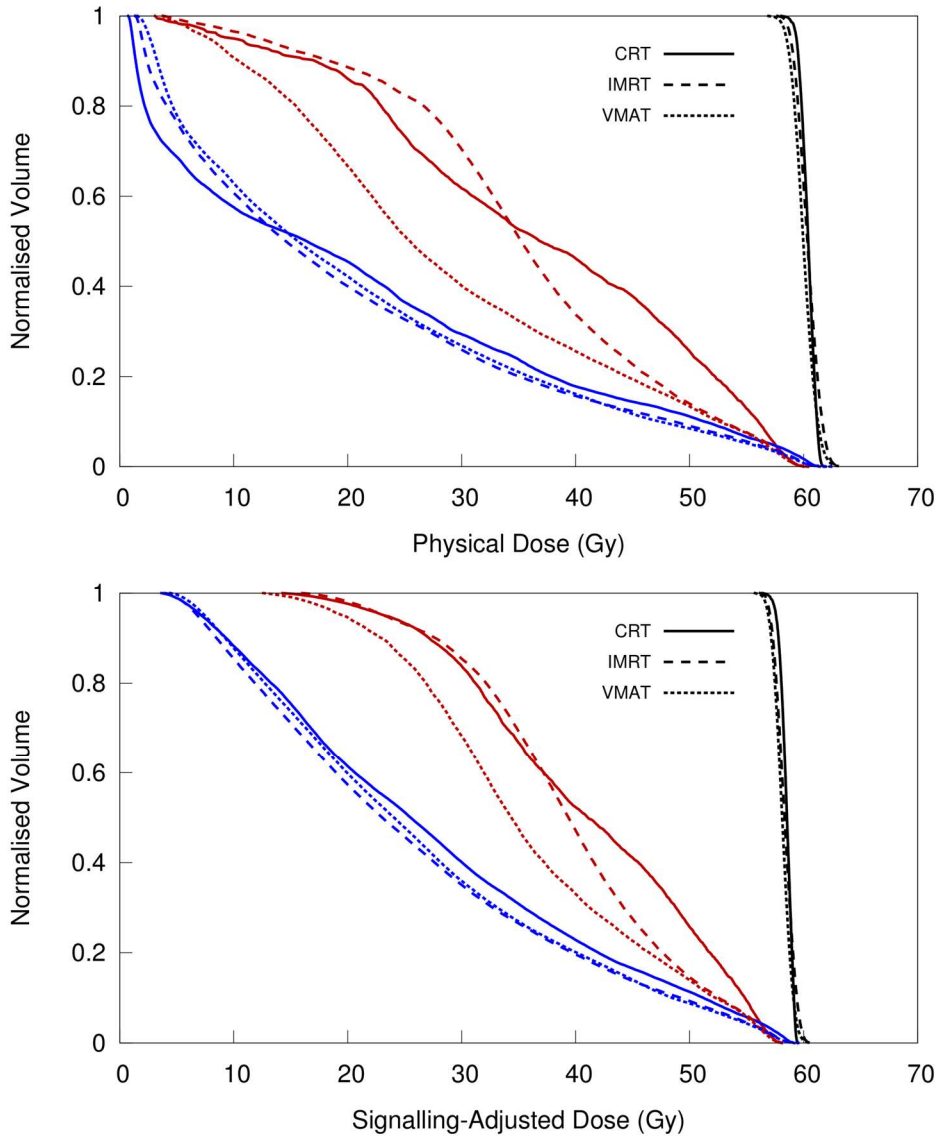

Figure 3: *Comparison of dose-volume histograms with and without a signalling component, averaged across 10 patients for CRT, IMRT and VMAT. Top: Physical DVHs for CRT (solid), IMRT (dashed) and VMAT (dotted) treatments, in bladder (blue), rectum (red) and target (black) volumes. Bottom: Signalling-adjusted DVHs for a signal range of 20 mm. It can be seen that these show significantly higher doses in low-dose regions, and significantly reduced differences between different plans.*

Impact on Dose Volume Histograms

Figure 3 presents dose-volume histograms averaged over all patients for the Planning Target Volume (PTV), rectum and bladder, shown for both physical dose and signalling-adjusted dose with a range of 20 mm.

As would be expected, the largest difference between physical and signalling-adjusted

doses is in the lowest dose regions (< 30 Gy), where communication from high-dose regions has the most significant impact, while in intermediate dose regions (30-50 Gy) there is a smaller effect. At the highest doses (>55 Gy) signalling-adjusted doses are actually smaller than the physical dose, typically by a few percent.

The impact of varying signal range on different treatments is illustrated in supplementary figure e2, showing that these effects build up rapidly at moderate ranges, but begin to saturate at higher ranges, as large portions of the volume are then entirely within the range of signalling from local dose maxima (particularly the case for the rectum, due to its proximity to the target volume).

Impact on Mean Dose & EUD

Figure 4 shows the change in mean dose and EUD for the three organs under consideration as a function of signal range for each different planning technique, again averaged across all patients.

In organs at risk it can be seen that there is a significant increase in mean dose, on the order of 7 Gy for the rectum and 10 Gy for the bladder. By contrast, the PTV sees a reduction in mean dose, up to nearly 3 Gy at 20 mm ranges. Due to the importance of high-dose regions in EUD calculations, the effect on these values is much less striking, with smaller increases in bladder EUD (n=0.5 (17)) and a shift to a small decrease in the rectum EUD (n=0.09 (18)).

Dosimetric Parameters

Table 1 presents a summary of dosimetric parameters for the Rectum, Bladder, and PTV. Again, it can be seen that there are dramatic increases in the fraction of organ at risk volumes exposed to low doses across all treatment plans. However, higher dose-levels

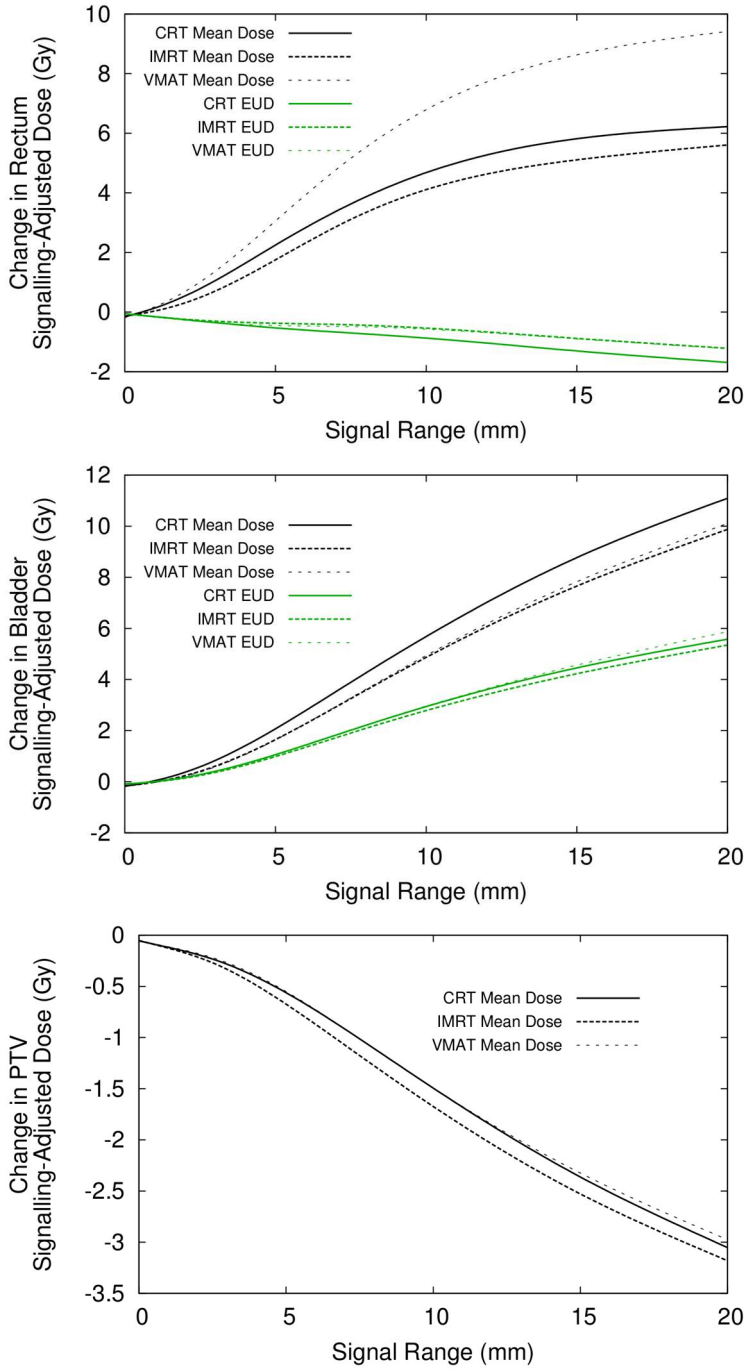

Figure 4: *Impact of signalling range on mean signalling-adjusted dose and EUD, for CRT, IMRT and VMAT plans calculated for rectum, bladder and prostate. For organs outside the treatment field, there is a significant increase in mean dose, while there is a smaller reduction in the mean target dose. However, these effects are reduced when EUD is considered, due to the greater emphasis on high-dose regions.*

which are typically used to evaluate treatment plans (e.g. V_{68}, V_{81}, V_{100}) are all much less affected, by at most a few percent. As a result, assessment of a given plan against these

metrics would not be significantly affected by whether physical or signalling-adjusted doses were considered. There is also typically a small decrease in the mean dose delivered to the target, on the order of 2 to 3 Gy, but this is uniform across all techniques.

Discussion

The implication that intercellular communication plays an important role at clinically-relevant doses is a significant departure from traditional radiobiology. Despite numerous *in vitro* results reporting these effects, a key question remains whether these observations are applicable to the *in vivo* conditions targeted in radiotherapy. One of the key initial tests of any model of the effects of intercellular communication is confirming that its predictions can be reconciled with clinical knowledge and practice.

Applying the theoretical model presented in this work leads to a distortion in dose distributions in organs near treatment fields which are exposed to low doses. This suggests that these effects may play a more important role in relatively parallel organs which are sensitive to lower dose regions (such as lung or bladder (17)). By contrast, these effects are much smaller in the high dose regions that are more significant in serial organs which are sensitive to dose hot-spots. Indeed, in organs which are both highly serial and exposed to a limited high dose region (such as the rectum), this actually translates into a reduction in EUD, which may sometimes prove significant in treatment planning, although this is typically small in magnitude. As these high dose regions are typically the constraints in therapy planning, assessment of different treatment plans in light of these effects leads to broadly similar conclusions as assessments based purely on physical dose, across all signal ranges.

Despite the limitations of the current model, this suggests that, even in the limit of relatively long signal ranges, the incorporation of a component of intercellular signalling leads to

similar predictions of cellular survival within the high-dose regions typically used to evaluate conventional radiotherapy plans. Thus, these radiation response models are not contradicted by comparison to clinical experience.

Similarly, this model and experimental results in modulated fields suggest an exponential dependence of damage resulting from intercellular communication, which translates into an approximately linear response in low-dose regions which see enough dose to drive signalling effects (e.g. 0.1 to 0.5 Gy per fraction (6, 15)). As a result, these effects are broadly compatible with the traditionally-assumed linear risk of cancer induction with dose (19) rather than introducing a strongly non-linear component at low doses which has sometimes been suggested.

The overall similarity of the conclusions drawn from physical and signalling-adjusted doses for different modalities is further emphasised by the similar optimisation criteria used in each of these planning approaches. The aim of a high, uniform target dose and minimal dose in surrounding healthy tissue means that the dose distributions in the vicinity of the target are broadly similar. As a result, all signalling-adjusted dose plans contain a similar, slowly-varying contribution in the vicinity of the target, which serves to reduce the distinction between different techniques (as seen in Figure 3). These effects mean that while there may be some improvements in predictive power from incorporating signalling into planning models, this is likely to be at the limits of clinical uncertainties for comparing different modalities used to deliver similarly-optimised plans.

However, intercellular signalling has the potential to play a much more significant role when comparing treatments which differ in other ways. For example, reduction of margins to take advantage of improved target delineation may have a negative impact on cell-killing at the tumour periphery. Similarly, the benefits of dose-painting or heavy ion therapies may

be significantly diminished if precisely targeted hot-spots within the tumour volume are blurred by signalling effects. Given interest in increasingly personalised treatment delivery, a more detailed understanding of these factors is necessary to fully optimise these techniques. This also offers a promising target for novel therapeutics, as it has been demonstrated that these effects can be inhibited both *in vitro* and *in vivo*, preferentially sparing out-of-field cells and those exposed to low doses.

Immediate clinical validation of these effects is likely to prove challenging. In addition to the relatively subtle variations suggested for the treatment plans considered in this work, the model presented here does not incorporate the impact of other factors which are known to influence therapeutic response, such regions of hypoxia, variation in the genetic profile of the cells within and around the tumour, and inter-fraction variation within the tumour. Any comprehensive model of radiation response must incorporate the relative effects of these parameters on both direct and signalling-driven responses, but this remains poorly quantified. Small-animal radiotherapy platforms (20) offer the possibility to probe these effects by delivering complex treatments to tumour-bearing animals with high precision to test potential impacts of intercellular communication in a more relevant system.

While the current model is sufficient for an initial theoretical evaluation of the impacts of intercellular signalling, there are still refinements required before it is in a position to generate clinical predictions. One of the most significant of these is a more accurate description of the signalling itself, as the current description of homogeneous signalling is clearly a simplification. Likewise, the range of these signals *in vivo* remains poorly characterised. While reports from *in vitro* skin models have suggested ranges on the order of 1 mm (21), there have also been reports of elevated cell killing outside treatment fields in Ptch1$^{+/-}$ mice, suggesting significantly longer signalling ranges (9). Additionally, the

signalling model in this work assumes that fractions are independent and identical. However, this validity of this assumption is much less sure for signalling-driven effects than for conventional exposures, as signalling effects may persist over time-frames longer than a single fraction, or be affected by changes in tumour size and composition through the treatment. Experiments to more precisely quantify all of these effects, both *in vivo* and *in vitro* would be a significant benefit to further development of this model.

Conclusions

Applying models developed to describe *in vitro* impacts of intercellular communication suggests that a significant proportion of the biological responses following radiotherapy result from intercellular communication, rather than direct damage. However, when physical and signalling-adjusted dose distributions are compared, it was found that predicted levels of survival were broadly similar in dose regions typically used to evaluate treatment plans, suggesting that these models can be reconciled with clinical experience.

Conflicts of Interest

The authors declare that no conflict of interest exists.

Acknowledgements

This work was supported by grants from Cancer Research United Kingdom (Grant no. C1513/A707 to KMP, and C212/A11342 for SMM and ARH). CKM is supported by a Health and Social Care Research and Development of the Public Health Agency training fellowship award.

Table 1: Dosimetric parameters comparing physically planned doses with signalling-adjusted doses for bystander signals of range 20 mm. Values are medians across the 10 patients. V_x=percentage of the organ exposed to X% of the prescribed dose. EUD=equivalent uniform dose. CI = conformity index.

Table 1: Impact of intercellular signalling on dosimetric parameters

	CRT		IMRT		VMAT	
Rectum						
	Physical	D_s, Range 20 mm	Physical	D_s, Range 20 mm	Physical	D_s, Range 20 mm
V_{14} (%)	95.01	100.00	97.53	100.00	90.28	100.00
V_{27} (%)	90.14	100.00	93.64	100.00	75.04	99.67
V_{41} (%)	74.53	97.27	84.16	97.02	53.68	91.53
V_{54} (%)	53.15	76.02	61.78	79.65	37.22	59.46
V_{68} (%)	46.79	50.41	33.67	45.41	28.94	33.71
V_{81} (%)	37.41	36.41	18.41	18.28	17.82	18.34
V_{100} (%)	0.03	0.00	0.04	0.00	0.05	0.00
Mean Dose (Gy)	45.38	51.59	43.54	49.14	36.19	45.60
EUD (Gy)	62.63	60.95	58.88	57.66	58.40	57.17
Bladder						
V_{14} (%)	55.76	97.88	59.38	94.38	59.26	96.38
V_{27} (%)	51.25	79.88	45.13	71.63	47.89	73.76
V_{41} (%)	43.63	57.88	33.76	51.50	33.89	52.64
V_{54} (%)	27.63	38.88	22.38	33.26	22.26	32.26

V_{68} (%)	17.38	21.13	15.63	19.13	16.63	19.51
V_{81} (%)	14.01	14.51	10.88	11.13	11.14	11.64
V_{100} (%)	2.26	0.00	0.88	0.00	0.89	0.00
Mean Dose (Gy)	25.20	36.28	23.49	33.36	23.34	33.44
EUD (Gy)	34.91	40.48	32.65	37.99	32.18	38.05
PTV						
Min Dose (Gy)	71.84	69.22	71.49	68.95	70.65	68.30
Median Dose (Gy)	74.08	71.13	73.69	70.71	73.33	70.54
Mean Dose (Gy)	74.47	71.42	74.52	71.34	73.96	70.99
CI	2.04	2.18	1.71	1.88	1.76	1.92

References

1. Bentzen SM. Theragnostic imaging for radiation oncology: dose-painting by numbers. The lancet oncology. 2005;6:112–7.

2. Mackonis EC, Suchowerska N, Zhang M, et al. Cellular response to modulated radiation fields. Physics in medicine and biology. 2007;52:5469–82.

3. Butterworth KT, McGarry CK, Trainor C, et al. Out-of-Field Cell Survival Following Exposure to Intensity-Modulated Radiation Fields. International journal of radiation oncology, biology, physics. 2011;79:1516–1522.

4. Prise KM, O'Sullivan JM. Radiation-induced bystander signalling in cancer therapy. Nature reviews. Cancer. 2009;9:351–60.

5. Ebert M, Suchowerska N, Jackson M, et al. A mathematical framework for separating the direct and bystander components of cellular radiation response. Acta oncologica. 2010;49:1334–43.

6. McMahon SJ, Butterworth KT, McGarry CK, et al. A Computational Model of Cellular Response to Modulated Radiation Fields. International journal of radiation oncology, biology, physics. 2012;84:250–256.

7. McMahon S, Butterworth K, Trainor C. A Kinetic-Based Model of Radiation-Induced Intercellular Signalling. PloS one. 2013;8:e54526.

8. Blyth B, Sykes P. Radiation-Induced Bystander Effects: What Are They, and How Relevant Are They to Human Radiation Exposures? Radiation Research. 2011;176:139–157.

9. Mancuso M, Giardullo P, Leonardi S, et al. Dose and spatial effects in long-distance radiation signaling in vivo: implications for abscopal tumorigenesis. International journal of radiation oncology, biology, physics. 2013;85:813–9.

10. Partridge M. A radiation damage repair model for normal tissues. Physics in medicine and biology. 2008;53:3595–608.

11. Mastro AM, Babich MA, Taylor WD, et al. Diffusion of a small molecule in the cytoplasm of mammalian cells. Proceedings of the National Academy of Sciences of the United States of America. 1984;81:3414–8.

12. Khoo VS, Dearnaley DP. Question of dose, fractionation and technique: ingredients for testing hypofractionation in prostate cancer--the CHHiP trial. Clinical oncology. 2008;20:12–4.

13. McGarry CK, McMahon SJ, Craft D, et al. Inverse planned constant dose rate volumetric modulated arc therapy (VMAT) as an efficient alternative to five-field intensity modulated radiation therapy (IMRT) for prostate. Journal of Radiotherapy in Practice. 2013:1–11.

14. Trainor C, Butterworth KT, McGarry C. DNA Damage Responses following Exposure to Modulated Radiation Fields. PLoS ONE. 2012;7:e43326.

15. Butterworth KT, McGarry CK, Trainor C, et al. Dose, dose-rate and field size effects on cell survival following exposure to non-uniform radiation fields. Physics in medicine and biology. 2012;57:3197–206.

16. Kutcher G, Burman C, Brewster L, et al. Histogram reduction method for calculating complication probabilities for three-dimensional treatment planning evaluations. International Journal of Radiation Oncology, Biology, Physics. 1991;21:137–146.

17. Burman C, Kutcher GJ, Emami B, et al. Fitting of normal tissue tolerance data to an analytic function. International Journal of Radiation Oncology, Biology, Physics. 1991;21:123–135.

18. Michalski JM, Gay H, Jackson A, et al. Radiation dose-volume effects in radiation-induced rectal injury. International journal of radiation oncology, biology, physics. 2010;76:S123–9.

19. Brenner DJ, Doll R, Goodhead DT, et al. Cancer risks attributable to low doses of ionizing radiation: assessing what we really know. Proceedings of the National Academy of Sciences of the United States of America. 2003;100:13761–6.

20. Verhaegen F, Granton P, Tryggestad E. Small animal radiotherapy research platforms. Physics in medicine and biology. 2011;56:55–83.

21. Belyakov O V, Mitchell S a, Parikh D, et al. Biological effects in unirradiated human tissue induced by radiation damage up to 1 mm away. Proceedings of the National Academy of Sciences of the United States of America. 2005;102:14203–8.